ACTA MEDICA LITUANICA. 2013. Vol. 20. No. 2. P. 85–92

Development and investigation of skin melanoma phantoms for ultrasonic examination

Kristina Andrėkutė[1],

Ilona Subotinaitė[2],

Skaidra Valiukevičienė[2],

Renaldas Raišutis[1]

[1] Ultrasound Institute, Kaunas University of Technology

[2] Department of Skin and Venereal Diseases of Lithuanian University of Health Sciences

Background. The purpose of this study was to develop skin mimicking phantoms with melanoma-like insertion with acoustic properties similar to the human skin. In order to guarantee that these phantoms are suitable for mimicking of the skin, we measured their parameters with an ultrasonography tool and compared with the human skin properties measured by other authors.

Materials and methods. Distilled water, gelatin and Intralipid® 20% IV fat emulsion were mixed in different proportions thus manufacturing four models of the skin tissue. For melanoma-mimicking insertion only gelatin and distilled water were used. Ultrasonic examinations of manufactured phantoms were performed with the ultrasound system DUB-USB equipped with a mechanically scanned single-element focused transducer.

Results. The speed of sound and the attenuation coefficient of all the manufactured phantoms were evaluated. This study demonstrates that the speed of sound decreases increasing concentration of Intralipid and it is close to the human skin tissue. The ultrasound velocity in the phantom material varied from 1 533.9 m/s up to 1 565.8 m/s depending on Intralipid fat emulsion concentration. The ultrasound velocity in the melanoma-like insertion was 1 602.4 ± 23.5 m/s (mean ± SD). It was also found that the concentration dependent magnitude of attenuation increment matched the theoretically defined tendency. The attenuation in the range of 0.15–0.4 dB/mm/MHz was estimated in the phantoms possessing different concentrations of Intralipid. The attenuation in the melanoma-like insertion region was 0.16 ± 0.02 dB/mm/MHz (mean ± SD). The magnitude of the attenuation coefficient is close to the attenuation in the human tissue.

Conclusions. The four skin tissue mimicking phantoms were developed and their acoustic properties were estimated during this study. The investigation showed that the estimated speed of sound and the attenuation coefficient were close to the values being estimated in the human skin tissue. Furthermore, it was noted that the acoustic properties could be controlled by changing the concentration of Intralipid and such a flexible phantom could be used for mimicking of the external tissue of the human body.

Key words: tissue mimicking phantom, ultrasonic properties, speed of sound, attenuation

Correspondence to: Kristina Andrėkutė, Ultrasound Institute, Kaunas University of Technology, Studentų 50, LT-51368 Kaunas, Lithuania. E-mail: kristina.andrekute@stud.ktu.lt

INTRODUCTION

Skin melanoma is a malignant tumor that arises from melanocytic cells and primarily involves the human skin (1). Even small tumors may have a tendency towards metastasis and thus a relatively unfavourable prognosis. Melanomas account for 90% of the deaths associated with cutaneous tumours (1, 2). Diagnosis of primary melanoma is based on early observation of clinical features and thickness, which are an important biomarker for the prognosis of the disease (1, 3, 4). The non-invasive ultrasonic diagnostics of melanoma is not always easy and is related to the experience of the clinician, accuracy of the imaging systems or image processing algorithms. Due to this reason a lot of new devices have been introduced in experimental stages for non-invasive diagnosis of skin lesions (5). In medical imaging it is necessary to have suitable phantoms, which might mimic the characteristics of the real skin. Phantoms are commonly used in the development of imaging systems and evaluation of image processing algorithms used for recognition or extraction of suspicious regions. A tissue-mimicking phantom emulates important properties of biological tissue for the purpose of providing a more clinically realistic imaging environment (5). In ultrasound imaging the most important phantom properties are the material's speed of sound and the acoustic attenuation coefficient (5). It is assumed that in the soft tissue the average speed of sound is 1 540 m/s (5, 6), the attenuation coefficient have been shown to be frequency-dependent (5, 7–9). It was demonstrated that the average value of attenuation in healthy human dermis at the forearm region is 0.21 dB/mm/MHz (in the frequency range of 14–50 MHz) (9). Both ultrasound velocity and attenuation are related to collagen content in the skin tissue (4, 9).

Previous studies (5, 7, 10, 11) have shown that hydrogels can be efficiently used for tissue-mimicking phantom design. The hydrogel phantoms are attractive for biomedical applications due to their mechanical properties. Other authors developed the skin phantoms for investigation of other non-invasive techniques (12, 13). Mazolli et al. manufactured optical skin phantoms with different thickness of melanoma-like insertion and tried to mimic the optical absorption and scattering (12). However, until now the ultrasonic skin phantom mimicking pigmented skin lesion has not been created and acoustic properties have not been investigated.

The purpose of this study was to develop the skin mimicking phantoms with melanoma-like insertion with acoustic properties similar to the human skin. In order to guarantee that these phantoms are suitable for the skin mimicking, we measured their parameters with an ultrasonography tool.

MATERIALS AND METHODS

In this study the skin phantoms for experimental ultrasonic investigation were manufactured by using three different ingredients listed in Table 1. Distilled water, gelatine and Intralipid® 20% IV fat emulsion (Fresenius Kabi, Austria) were mixed in different proportions thus manufacturing different four models of the skin tissue.

The mixtures were poured into Petri dishes and were placed into a cold chamber (T = 5 °C) for about 20 minutes. The horizontal position of each dish was followed precisely using the levels. The mixtures were taken out when the solid state was achieved. We used a scalpel to make cylindrical holes of approximately 5 mm diameter and 3.8 mm thickness (up to the bottom of the dish). In the next stage the melanoma mimicking material was prepared. It was known that melanomas appear

Table 1. Concentrations of the ingredients used for manufacture of skin phantoms

Phantom	Water, % ($m_w/m_{general}$)	Intralipid, % ($m_i/m_{general}$)	Gelatin, % ($m_g/m_{general}$)	Density, g/ml
I	46	40	14	1.0742
II	36	50	14	1.052
III	26	60	14	1.0226
IV	16	70	14	1.0176
Insertion	83	–	17	0.976

like anechoic structures in B-mode ultrasound images and accordingly only water and gelatine were mixed for mimicking melanoma-like insert. The melanoma mimicking mixtures were poured into the cylindrical holes which were made in the centres of the skin tissue mimicking phantoms. The melanoma-mimicking insertion was coloured by using liquid Indian ink (negligible amount to compare with the concentrations of the main ingredients) in order to separate visually the insertion from the surrounding media. Finally, phantoms were placed horizontally for cooling again. Therefore, the uniform thickness of the phantom was achieved.

The ultrasound system DUB-USB (Taberna Pro Medicum, Luneburg, Germany) equipped with a mechanically scanned single element focused transducer (central frequency of 22 MHz, bandwidth approximately 12–28 MHz, focal depth of 11 mm) was used for ultrasonic examinations of manufactured skin melanoma mimicking phantoms. The pulse-echo experimental set-up is shown in Fig. 1. The ultrasound beam was focused at the surface of the phantom as shown in Fig. 1.

The ultrasonic transducer was in the perpendicular position during scanning of all four phantoms. The lateral scanning width was 12.8 mm, the scanning step was 0.033 mm and

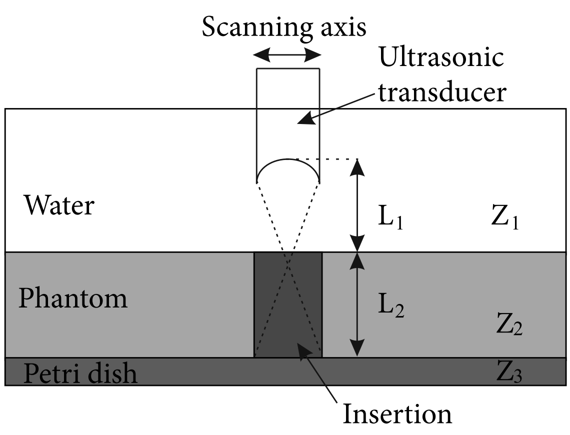

Fig. 1. Experimental set-up for the speed of sound measurements. The average thickness of the phantom (L_2) was 3.8 ± 0.56 mm, the distance up to the focus (L_1) 11 mm, all three materials had different acoustic impedances – Z_1 (acoustic impedance of water), Z_2 (acoustic impedance of phantom), Z_3 (acoustic impedance of Petri dish)

382 A-scans of each phantom were acquired. The scanning duration was less than 0.4 sec per single B-scan. The radio-frequency echo signals were digitized by a 8-bit A/D converter at 100 MHz sampling rate and stored on the hard disk of a personal computer.

The acoustic properties (speed of sound and attenuation) of the phantoms were investigated. For accurate determination of the speed of sound in the layers of the phantom, the reference ultrasound time of flight (TOF) was measured by using the ultrasound system and a tank containing distilled water. The speed of sound (c_{ph}) was determined by measuring the duration between the echoes reflected from the surface of the Petri dish (in the case of the phantom and in the case of the insertion filled with distilled water only) and the surface of the phantom could be expressed by the following formula (5, 14):

$$c_{ph} = \frac{2L_2}{\Delta t_{ph}} = \frac{c_w \Delta t_w}{\Delta t_{ph}};\ L_2 = \frac{c_w \Delta t_w}{2}, \qquad (1)$$

where c_{ph} is the speed of sound in the phantom, c_w = 1 490.2 m/s (measurements were performed at 22.8 °C ± 0.5 °C temperature) is the temperature-dependent speed of sound in the distilled water, L_2 is the thickness of the phantom, Δt_w and Δt_{ph} are TOF of ultrasound in the water and the phantom, respectively. The speed of sound in the insertion (c_i) was evaluated at the same thickness as in the phantom (L_2). A convex deformation of the insertion surface appeared due to the tension which occurs during the cooling (see Fig. 2D). Thickness of the insertion ($L_i = c_i \Delta t_i /2$) was evaluated by summing the thickness of the phantom (L_2) and the thickness of deformation through which TOF is Δt_{def}.

The frequency-dependent ultrasound attenuation can be estimated by using Fourier analysis of the signals. The ultrasound attenuation coefficient was estimated according to the following equation (15, 16):

$$\alpha_{ph}(f) = -\frac{20}{2L_2} \log_{10} R \frac{A(f)}{A_0(f)}, \qquad (2)$$

where $\alpha_{ph}(f)$ is the frequency-dependent ultrasound attenuation of the phantom in dB/mm, R is the total reflection coefficient at the water-phantom and phantom-dish interfaces, $A(f)$ is the magnitude of the spectrum of echo reflected from the water-phantom interface, $A_0(f)$ is the magnitude of the spectrum of echo reflected from the phantom-Petri dish interface, L_2 is the thickness of the phantom in mm. The echo-signals from the phantom surface and the phantom bottom were gated using the Hamming window before application of the fast Fourier transform. The calculated $\alpha_{ph}(f)$ dependences were linearly approximated. The regression lines were obtained using the method of least squares fitting.

The acoustic energy is reflected when the ultrasound waves penetrate through the layers having different acoustic impedances. The impedance $Z = \rho c$ depends on the ultrasound velocity (c) and density (ρ) of the scanned media (7). The acoustic reflection coefficient of ultrasonic waves from the surface of the phantom R_{12} (water-phantom interface) can be expressed as follows (7):

$$R_{12} = \frac{Z_2 - Z_1}{Z_2 + Z_1}, \quad (3)$$

where Z_1 and Z_2 are the acoustic impedances of water and the phantom, respectively. The transmission coefficient of ultrasonic waves through the water-phantom interface (T_{12}) can be expressed by the following formula:

$$T_{12} = \frac{2 \cdot Z_1}{Z_2 + Z_1}. \quad (4)$$

The total reflection coefficient in the three layer medium was expressed as follows:

$$R = \frac{R_{12}}{T_{12} \cdot T_{21} \cdot R_{23}}, \quad (5)$$

where R_{23} is the reflection coefficient of ultrasonic waves reflecting from the interface between the phantom and the Petri dish (calculated in a similar way as (3)) and T_{21} is the transmission coefficient of ultrasonic waves through the phantom-water interface. The density of the Petri dish is 1.18 g/ml and the speed of sound is 2 672 m/s (Petri dish material poly(methyl methacrylate)) (17).

RESULTS

The speed of sound and the attenuation coefficient of all the manufactured phantoms were evaluated. The acquired ultrasound B-scans and A-scans signals which were used for the evaluation are presented in Fig. 2.

The ultrasound velocity dependence on Intralipid fat emulsion concentration is presented in Fig. 3. The ultrasound velocity in the phantom material varies from 1 533.9 m/s up to 1 565.8 m/s depending on Intralipid fat emulsion concentration. The ultrasound velocity in the melanoma-like insertion was 1 602.4 ± 23.5 m/s (mean ± SD). As expected, it was observed that the speed of sound decreases increasing concentration of Intralipid. Accordingly, this acoustic property could be controlled in the process of physical modeling of the human skin. It could be noticed that the speed of sound in the tissue mimicking phantom is close to that of the real skin tissue (Table 2).

The acoustic attenuation was determined in the range from 12 up to 28 MHz. Fig. 4 shows the dependence of the attenuation versus frequency in skin tissue phantoms with different concentrations of Intralipid and insertion. It could be summarized that the concentration dependent magnitude and the slope of attenuation increment match the theoretically defined tendency. Attenuation in the range of 0.18–0.4 dB/mm/MHz was estimated in the phantoms with different concentrations of Intralipid. An attenuation in the melanoma-like insertion region was 0.16 ± 0.02 dB/mm/MHz

Table 2. Comparison of acoustic properties of the phantoms and properties of the skin

	Speed of sound, m/s	**Attenuation coef., dB/mm/MHz**
Phantom I	1 565.8	0.18
Phantom II	1 560.1	0.28
Phantom III	1 556.4	0.32
Phantom IV	1 533.9	0.41
Insertion	1 602.4 ± 23.5	0.16 ± 0.02
Human skin	Epidermis 1 540; dermis 1 580 (8)	0.21 (9)
Melanoma	1 553–1 588 (14)	Undetermined

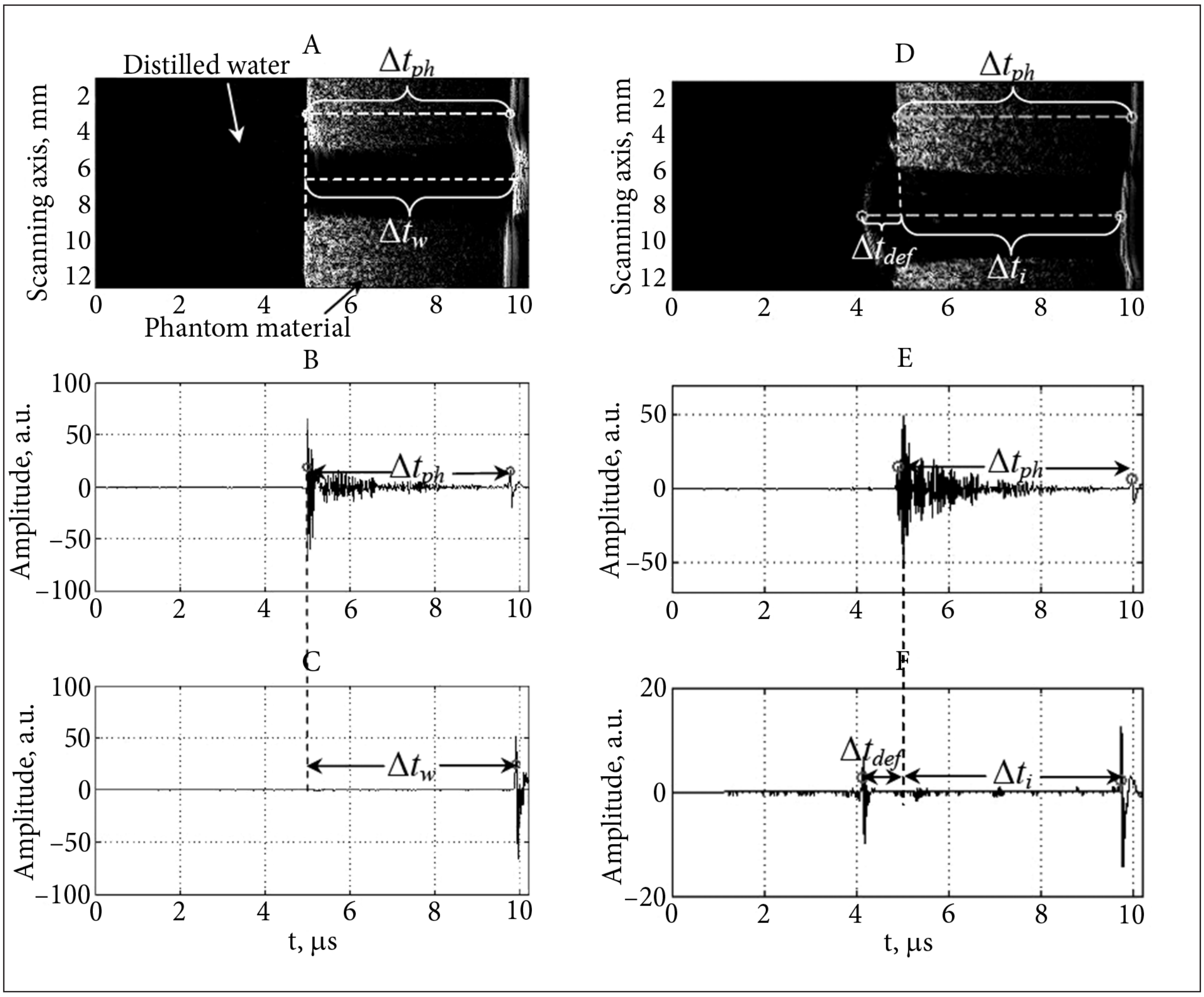

Fig. 2. Ultrasound B-scan images and A-scan signals of the phantoms: A – the B-scan image of the region with a cylindrical hole containing distilled water; B – the reflected A-scan signal from the water-phantom interface; C – the reflected A-scan signal from the water-dish interface; D – the B-scan image of the region with the melanoma-like insertion; E – the reflected A-scan signal from interfaces of the phantom; F – the reflected A-scan signal from interfaces of the insertion region. The circles placed on B-scans and A-scans denote the boundaries of the phantom which were detected by the amplitude threshold of the reflected ultrasonic waves

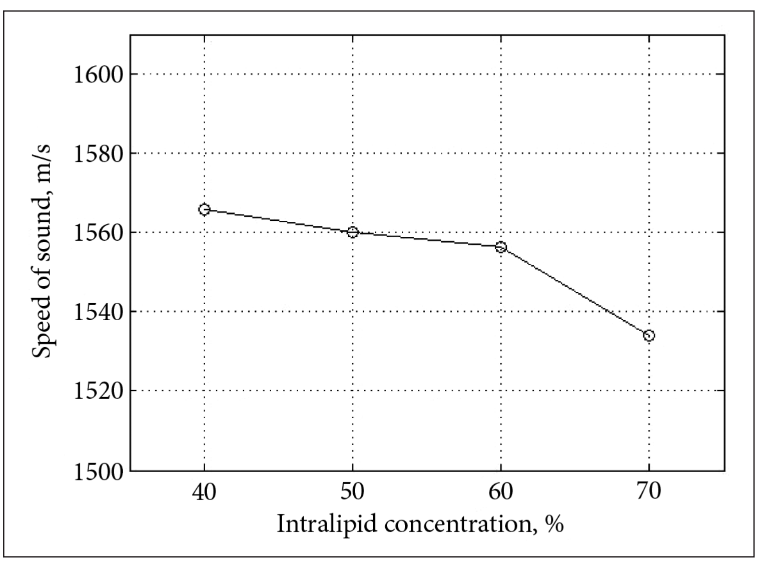

Fig. 3. The relationship between ultrasound velocity in the phantoms and differences of Intralipid fat emulsion concentration

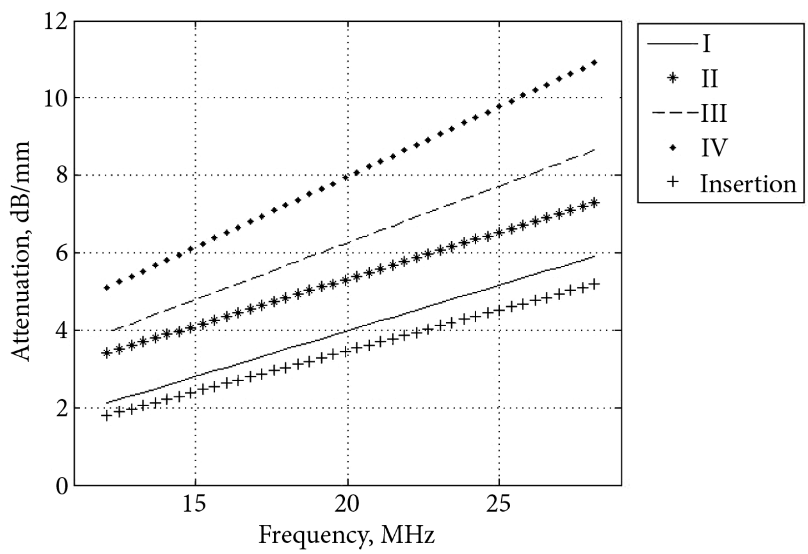

Fig. 4. The relationship between the ultrasound attenuation in the phantom and ultrasound frequency. The legend indicates different scanned mediums: the phantoms with different Intralipid fat emulsion concentration (Table 1) and the melanoma-like insertion

(mean ± SD). The magnitude of the attenuation coefficient is close to that of the human tissue measured by other authors (5, 8, 9).

DISCUSSION AND CONCLUSIONS

The four skin tissue mimicking phantoms were developed and their acoustic properties were estimated during this study. The investigation showed that the estimated speed of sound and the attenuation coefficient were close to the values being estimated in human skin tissues. Furthermore, it was noted that the acoustic properties could be controlled by changing concentration of Intralipid and such a flexible phantom could be used for mimicking of various areas of the human body. These phantoms will be used in development and evaluation of the measurement methods and image processing algorithms in further studies with the aim to perform the early stage melanoma detection and evaluation.

A limitation of this study is that only four phantoms with different concentrations were manufactured and investigated. The repeatability of phantom properties will be estimated in forthcoming studies when the acoustic properties of a few phantoms having the same content will be estimated. Also, long-term stability of the acoustic properties of the phantoms was not evaluated in this study. Usually, phantoms should be stored at low temperatures for maintaining their mechanical stability since gelatin dissolves in a warm environment. But it should be mentioned that our expectation was to manufacture the phantom to be used for acquisition of B-mode images which will be pressed further, therefore it is sufficient if the phantom will be stable as long as the scanning data of B-mode image will be recorded.

Our gelatin based phantoms have a potential to be the promising tools not only for preclinical ultrasonic investigations of the skin melanoma, but also for other soft tissue lesions as they possess echogenic properties that would make them ultrasonically detectable.

ACKNOWLEDGEMENTS

This work was partially sponsored by the Agency for International Science and Technology Development Programmes in Lithuania under the Eurostars Project SKINMONITOR “Diagnosis of Skin Cancer Based on Information and Communication Technologies Tools”.

Received 4 April 2013
Accepted 27 June 2013

References

1. Garbe C, Peris K, Hauschild A, Saiag Ph, Middleton M, Spatz A, et al. Diagnosis and treatment of melanoma: European consensus-based interdisciplinary guideline. Eur J Cancer. 2010; 46(2): 270–83.

2. Garbe C, Leiter U. Melanoma epidemiology and trends. Clin Dermatol. 2009; 27(1): 3–9.
3. Kaikaris V, Samsanavičius D, Maslauskas K, Rimdeika R, Valiukevičienė S, Makštienė J, Pundzius J. Measurement of melanoma thickness – comparison of two methods: ultrasound versus morphology. J Plast Reconstr Aesthet Surg. 2011; 64(6): 796–802.
4. Jasaitiene D, Valiukeviciene S, Linkeviciute G, Raisutis R, Jasiuniene E, Kazys R. Principles of high-frequency ultrasonography for investigation of skin pathology. J Eur Acad Dermatol Venereol. 2011; 25: 375–82.
5. Cook JR, Bouchard RR, Emelianov SY. Tissue-mimicking phantoms for photoacoustic and ultrasonic imaging. Biomed Opt Express. 2011; 2(11): 3193–206.
6. Serup J, Keiding J, Fullerton A, Gniadecka M, Gniadecki R. High-frequency ultrasound examination of the skin: introduction and guide. In: Serup J, Jemec GBE, editors. Handbook of Non-Invasive Methods and the Skin. Boca Raton: CRC Press; 1995.
7. Browne JE, Ramnarine KV, Watson AJ, Hoskins PR. Assessment of the acoustic properties of common tissue-mimicking test phantoms. Ultrasound Med Biol. 2003; 29(7): 1053–60.
8. Guittet Ch, Ossant F, Vaillant L, Berson M. *In vivo* high-frequency ultrasonic characterization of human dermis. IEEE Trans Biomed Eng. 1999; 46(6): 740–6.
9. Raju BI, Srinivasan MA. High-frequency ultrasonic attenuation and backscatter coefficients of *in vivo* normal human dermis and subcutaneous fat. Ultrasound Med Biol. 2001; 27(11): 1543–55.
10. Zell K, Sperl JI, Vogel MW, Niessner R, Haisch C. Acoustical properties of selected tissue phantom materials for ultrasound imaging. Phys Med Biol. 2007; 52: 475–84.
11. Madsen EL, Zagzebski JA, Banjevie RA, Jutila RE. Tissue mimicking materials for ultrasound phantoms. Med Phys. 1978; 5(5): 391–4.
12. Mazzoli A, Munaretto R, Scalise L. Preliminary results on the use of a noninvasive instrument for the evaluation of the depth of pigmented skin lesions: numerical simulations and experimental measurements. J Lasers Med Sci. 2010; 25(3): 403–10.
13. Wang T, Mallidi S, Qiu J, Ma LL, Paranjape AS, Sun J, et al. Comparison of pulsed photothermal radiometry, optical coherence tomography and ultrasound for melanoma thickness measurement in PDMS tissue phantoms. J Biophotonics. 2011; 4(5): 335–44.
14. Weichenthal M, Morh P, Breitbart EW. The velocity of ultrasound in human primary melanoma tissue – implications for the clinical use of high resolution sonography. BMC Dermatol. 2001; 1: 1. Available from: http://www.biomedcentral.com/1471-5945/1/1
15. Godechal Q, Leveque P, Marot L, Baurain JF, Gallez B. Optimization of electron paramagnetic resonance imaging for visualization of human skin melanoma in various stages of invasion. Exp Dermatol. 2012; 21(5): 341–6.
16. Wang T, Mallidi S, Qiu J, Ma LL, Paranjape AS, Sun J, et al. Comparison of pulsed photothermal radiometry, optical coherence tomography and ultrasound for melanoma thickness measurement in PDMS tissue phantoms. J Biophotonics. 2011; 4(5): 335–44.
17. Bochud N, Rus G. Probabilistic inverse problem to characterize tissue-equivalent material mechanical properties. IEEE Trans Ultrason Ferroelec Freq Control. 2012; 59(7): 1443–56.

Kristina Andrėkutė, Ilona Subotinaitė, Skaidra Valiukevičienė, Renaldas Raišutis

ODOS FANTOMŲ SU MELANOMĄ IMITUOJANČIU INTARPU SUKŪRIMAS IR IŠTYRIMAS ULTRAGARSINE SISTEMA

Santrauka

Tikslas. Šio tyrimo tikslas buvo sukurti odą imituojantį fantomą su melanomą imituojančiu intarpu, kurio akustinės savybės būtų artimos žmogaus odos savybėms. Tam, kad įsitikintume, ar šie fantomai tinkami odos imitavimui, mes pamatavome parametrus ultragarsine sistema.

Medžiagos ir metodai. Keturių odos fantomų gamybai skirtingomis proporcijomis buvo sumaišyti distiliuotas vanduo, želatina ir Intralipid® – 20 % IV riebalų emulsija. Melanomai imituoti naudojome tik želatiną ir distiliuotą vandenį. Pagaminti fantomai ištirti ultragarsine sistema DUB-USB su mechaninio nuskaitymo keitikliu.

Rezultatai. Visuose pagamintuose fantomuose buvo įvertinti ultragarso bangų greitis ir slopinimo koeficientas. Tyrimas rodo, kad ultragarso greitis mažėja didėjant Intralipido koncentracijai ir yra artimas greičiui žmogaus odoje. Ultragarso greitis fantomo medžiagoje kito nuo 1 533,9 m/s iki 1 565,8 m/s priklausomai nuo Intralipido koncentracijos. Ultragarso greitis melanomą imituojančiame intarpe buvo 1 602,4 ± 23,5 m/s. Nustatyta, kad slopinimo vertė priklauso nuo Intralipido koncentracijos ir atitinka teorinę slopinimo reikšmę žmogaus audiniuose. Slopinimas fantomuose su skirtingomis Intralipido koncentracijomis buvo nuo 0,15 iki 0,4 dB/mm/MHz, o melanomą imituojančiame intarpe – 0,16 ± 0,02 dB/mm/MHz.

Išvados. Tyrimo metu nustatyta, kad apskaičiuotos ultragarso greičio ir slopinimo koeficiento vertės yra artimos tikrų odos audinių vertėms. Be to, akustines savybes galima kontroliuoti keičiant intralipido koncentraciją, o tokie lengvai pritaikomi fantomai gali būti naudojami imituojant įvairių žmogaus kūno vietų paviršinius audinius.

Raktažodžiai: odą imituojantis fantomas, akustinės savybės, ultragarso greitis, slopinimas